Proceedings of the Korean Nuclear Society Spring Meeting

Cheju, Korea, May 2001

The Influence of Delta(ä) Ferrite on the Irradiation Effects in Type 304 Stainless Steel Weldment

Se-Hwan CHI, Gen-Chan Kim[1], Jun-Hwa Hong

Nuclear Materials Development Team, Korea Atomic Energy Research Institute

P.O Box 105, Yusong, Taejon, 305-600, South Korea

Yong-Kwan Shin*,Young-Jik Kim

Department of Advanced Materials Engineering, Sungkyunkwan University,

Chongchon-dong, Suwon, Kyonggi-do, 400-746, South Korea

Abstract

Differences in the high energy ion induced defects microstructure of BCC ä-ferrite and FCC austenite matrix, and the effects of ä-ferrite on the Vickers micro-hardness increase after irradiation were investigated for Type 304 stainless steel weldments containing two different ä-ferrite contents **:** ferrite number(FN) 5.5 and 8.5, respectively. Specimens were irradiated to 1.5 dpa by 8 MeV Fe^{+4} ions using a Tandem Vande-Graff accelerator (flux: 4.3 x 10^{10} ion/cm^2.sec, fluence : 0.83 x 10^{15} ion/cm^2) at room temperature. TRIM 95 results showed that a peak damage appeared at 1.5 ㎛ in depth with 0.7㎛ full width at half maximum (FWHM), and these results could have been confirmed by TEM on irradiation induced defects (IID) distribution. Clear differences in the size and number of IID in the form of black dots (size: 5 – 10 nm) and loops were observed between the austenitic matrix and ä-ferrite, where the size of IID was far larger in FCC matrix than BCC ä-ferrite. Vickers micro-hardness (Hv) test results showed that ä-ferrite has increased about five times higher than austenitic matrix after irradiation. This observation was used to explain the higher Vickers micro-hardness increase due to irradiation in the high FN weldment than the lower FN weldment, i. e., 44 % increase for 8.5 FN to 36% increase for 5.5 FN after irradiation.

[1] On leave from Institute of Nuclear Physics of Uzbekistan Academy of Science, Uzbekistan.

* Hyun-Dai Motors

1. Introduction

Currently, in relation to the residual delta(ä)-ferrite in the austenitic stainless steel weldment after the welding of austenitic stainless steel core support structures and Class 1 and 2 components in Section III, ASME boiler and pressure vessel code, the ferrite content in the weld filler metal is required as depicted by a ferrite number(FN) to be between 5 and 20. This lower limit provides sufficient ferrite to avoid microfissuring in weld, whereas the upper limit provides a ferrite content adequate to offset dilution **[1].** Thus, the upper limit is to minimise embrittlement in service and the lower one to prevent solidification cracking of the weld during the component fabrication.

Contrary to these beneficial effects of the ASME specified delta(ä)-ferrite content in the austenitic stainless steel weld, however, some detrimental effects are expected due to the difference in the crystal structure between the bcc delta(ä)-ferrite and fcc austenite matrix, especially under the irradiation condition, since significant differences in the radiation sensitivity between the fcc and bcc crystal have been observed by the computer simulation or experimental studies **[2][3][4][5][6].**. In this sense, since the integrity of the stainless steel weld is very important in the nuclear components, it is necessary to evaluate the role of delta(ä)-ferrite in the stainless steel welds under irradiation condition as an input for the safety evaluation of the component.

In the present study, using two nuclear grade austenitic stainless steel welds of different delta(ä)-ferrite content, the influence of delta(ä)-ferrite on the irradiation effects in type 304 stainless steel weld was studied through the investigation of the differences in the irradiation-induced defect microstructure of bcc delta(ä)-ferrite and fcc austenitic stainless steel weld matrix, and by identifying the contribution of bcc delta(ä)-ferrite to the irradiation-induced increase in the Vickers microhardness of the weld.

2. Experimental

2.1 Material and specimen

Two weld coupons, ferrite number(FN) 5.5 and 8.5, were prepared by combination of two filler metals: 308 L or 308L plus 309L**,** and two different welding methods: submerged arc welding(SMAC) or Flux cored arc welding (FCAC) **[7]**. From the coupons, specimens for microstructure investigation (unirradiated and irradiated, and optical and transmission electron microscope(TEM)) and Vickers microhardness measurement were prepared. All the specimen surface for Vickers microhardness and accelerator irradiation were prepared by electropolishing using a solution made of acetic acid (95ml) and perchloric acid (5 ml).

Before and after machining specimens from the coupons, Ferrite Content Meter (model 1.054) was used to identify and grouping the specimens by the FN. Chemistries of the type 304 stainless steel plate and filler metals are shown in **Table 1 ~ 3.** **Fig. 1** shows optical micrographs for the weldments prepared with two different FN.

2.2 Irradiation and TRIM calculation

Tandem Vande-Graaff accelerator was used for the irradiation of 8 MeV Fe^{+4} ions to 1.5 dpa on the prepared specimens (1.3 x 10 x 0.5 mm). Beam current was 250 nA (flux: 4.3 x 10^{10} ions.cm^{-2}.S^{-1}, fluence: 0.83 x 10^{15} ioncm^{-2}), and irradiation time determined by TRIM 95 under the present irradiation condition was about 20,000 sec. Irradiation temperature was not over 60 ℃. Density and number of atoms in unit volume used for the calculation were 8.0 g/cm^3 and 8.72 x 10^{22} atoms per cm^3, respectively. If possible, relevant ASTM E 521-96 procedure and parameters were followed during the irradiation **[8]**.

2.3 Microstructure investigation

Optical, scanning electron microscopy (SEM) and transmission electron microscopy (TEM) were performed for delta(ä)-ferrite microstructure (size and morphology), and irradiation-induced defect microstructure and diffraction pattern analysis. For ion-irradiated specimens, TEM specimens for irradiation-induced defects microstructure investigation at a range were made by ion milling (Ar, 4.5 keV) the thin Fe and Ni plated specimen after irradiation. Details of the specimen preparation for TEM on the range are reported elsewhere **[9]**.

2.4 X-ray diffraction analysis

XRD analysis were performed to examine the possibility of new phase formation during irradiation using Cu-K_α source for 2 θ of 30 ~ 100 ° and 4 °/min scan speed.

2.5 Microhardness measurement

To evaluate the influence of delta(ä)-ferrite on the irradiation effects in the weld, Vickers microhardness(H_V)tests (tester model: Shimadzu HMV-2000) were conducted. In the present experimental condition, since the irradiation-induced defects as well as delta(ä)-ferrite affect the hardness, H_v test load was varied from 5 g to 1,000 g to control the indentation depth against the range. The contribution of delta(ä)-ferrite to the irradiation-induced Vickers microhardness increase in weld was evaluated by separating the contribution of delta(ä)-ferrite phase from the combined delta(ä)-ferrite and austenite matrix phase in the indentation area. Tests were conducted for 15 sec loading condition at room temperature.

3. Results and Discussion

3.1 Damage depth profile and defects size distribution

Fig. 2 shows the TRIM 95 result on the change of ion energy absorbed by recoil atoms with depth, where, the peak damage depth (range) appears at around 1.5 ㎛ with an about 0.7 ㎛ full with at half maximum (FWHM). **Fig. 3** shows the distribution of irradiation-induced defects (black dots and loops) by TEM. Good agreement between the calculation and actual distribution of defects was confirmed. High population of irradiation-induced defects were formed through out the matrix parallel to the ion incident surface forming a thick dark line irrespective of delta(ä)-ferrite content. The average size of the defects in the austenite weld matrix was 14.6 ± 10.2 nm, and was 6.4 ± 3.5 nm for delta(ä)-ferrite.

3.2 Differences in the irradiation-induced defects microstructure between the austenite matrix and delta(ä) ferrite

Fig. 4 shows the weld microstructures before and after irradiation both for delta(ä)-ferrite and austenite matrix by TEM. As expected, the as-received microstructure of delta(ä)-ferrite and austenite matrix showed no large difference in TEM as well as optical microstructure. However, in **Fig. 5**, it is seen that irradiation-induced defects (black dots, and black and white contrasts) are formed both in delta(ä)-ferrite and austenite matrix, and the size and density are far smaller and lower in delta(ä)-ferrite. Thus, a large amount of defects in size of 5 – 25 nm were found in the weld austenite matrix, while a little and smaller defects (about 43 % of the average defect size formed in fcc austenite weld matrix) were found in delta(ä)-ferrite.

These differences in the size and number density of irradiation-induced defects between the delta(ä)-ferrite and austenite matrix may be attributed to the difference in the defect accumulation rate between the fcc and bcc crystal structure. Clear differences have been reported between fcc and bcc in the defect accumulation behavior. Victoria et al suggested that nearly three orders of magnitude higher dose is needed to attain the same cluster density in bcc Fe than that in fcc Cu **[5]**.

The reason for the differences are not entirely clear at this point. However, reported studies for the differences indicate that, from the computer simulations of cascade evolution, while stable stacking fault tetrahedra (SFT) results from large cascades (for PKAs ~ 30 – 50 keV) in Cu **[10]**, interstitial loops resulting from the cascade quenching in Fe are much smaller and highly mobile **[11][12][13]**.

Regarding the type of the defects in **Fig. 5**, most of the defects in black and white contrasts appeared to be dislocation loops from the perpendicular relation between $\bar{\mathbf{g}}$ the operating reflection and the sense of the black-white contrast associated with the irradiation-induced

defects under the two beam condition **[14]**. Actually, the main population of defect clusters in the irradiated austenitic stainless steel of low stacking fault energy (SFE) are known as loops, even SFTs are observed with low SFE **[5]**.

3.3 Vickers microhardness change with crystal structure

Fig. 6 shows the increase in the Vickers microhardness after irradiation for each test load from 5 to 1,000g with the relative indentation position against the range. Calculation of indentation depth shows that, at the 5g load, indentation with the possible influence of loading resides within the highly damaged region (range plus FWHM) during the test. As expected, the increase in the Hv due to irradiation was the largest for the 5g test load irrespective of FN. It is seen that the higher the FN, the larger in the Hv due to irradiation. Thus, at 5g load, FN 8.5 weld has increased 10 % more than FN 5.5 in H_V after irradiation.

To investigate the effects of different phase, thus, different crystal structure of fcc austenite matrix and bcc delta(ä)-ferrite in weld, on the Hv increase due to irradiation, all the indentation made in **Fig. 6** were measured in area dividing into two phases of different crystal structure. Here, seventy Hv indentation were made on the two phase as-received and irradiated specimens, respectively, **Fig. 7**. In average, the area of delta(ä)-ferrite was about 25% of the 5g load indentation.

From the measurements on the indented area with or without delta(ä)-ferrite phase, **Fig. 7**, the increase in the Hv in austenite matrix due to irradiation, $\triangle H_{v\gamma}$, was measured to be about 28 in average, and the increase in Hv in the area with two phase, $\triangle Hv_{\delta+\gamma}$, was measured to about 45 in average. From the consideration of the average delta(ä)-ferrite area in the two phase indentation, the ratio of the irradiation-induced increase in Hv for each phase, $\triangle Hv_{\delta} / \triangle Hv_{\gamma}$, was determined to be **5**. Thus, the bcc delta(ä)-ferrite appeared to harden five times higher than the fcc austenite matrix under the present experimental condition.

The present higher hardening behavior in bcc delta(ä)-ferrite to fcc austenite matrix may be understood by the differences in the irradiation-induced defects microstructure. Recent studies on the differences due to crystal structure show that there are differences in the defect cluster size distribution, defect accumulation behavior, the migration mechanism of self-interstitial atom(SIA), the fraction of glissile SIA clusters produced in the cascades, and the interaction of dislocation with glissile defect clusters **[4**]. The invisible irradiation-induced defects in the bcc delta(ä)-ferrite in **Fig. 5 (b)** by TEM, even its five times higher increase in Hv to fcc austenite matrix under the same irradiation condition, seem to be a characteristics of bcc crystal structure. Currently, in bcc reactor pressure vessel steels, defects invisible by TEM due to its fine size (~ < 5 nm) are characterized by SANS and AP/FIM **[15]**.

In the present study, all the increase in the Vickers microhardness can be attributed to the

hardening due to irradiation-induced defects since no new phase was formed by irradiation as confirmed by the X-ray diffraction (XRD), **Fig. 8.**

4. Conclusion

The influence of delta(ä)-ferrite on the irradiation effects in Type 304 stainless steel weld was investigated for specimens of two different delta(ä)-ferrite contents, ferrite number 5.5 and 8.5, after irradiation to 1.5 dpa by 8 MeV Fe^{+4} ions. Following conclusions were made.

(1) Distribution of irradiation-induced defects observed by TEM agreed well with those of TRIM95 calculation. The peak damage (Range) appeared at around 1.5 ㎛ in depth with an about 0.7 ㎛ full with at half maximum (FWHM). From the comparison of the size and density of irradiation-induced defects between the fcc austenite matrix and bcc delta(ä)-ferrite, a higher defect accumulation rate in fcc weld matrix was confirmed.
The average defects size in fcc austenite matrix was about 2.3 times larger to those of bcc delta(ä)-ferrite.

(2) From the perpendicular relationship between $\bar{\mathbf{g}}$ the operating reflection and the sense of black and white contrast, most of irradiation-induced defects were analyzed to be dislocation loops irrespective of crystal structure.

(3) The bcc delta(ä)-ferrite appeared to harden five times higher than the fcc austenite matrix under the same irradiation condition. With this reason, the FN 8.5 weld seems to show a higher Vickers microhardness than the FN 5.5 weld.

Acknowledgement

The authors wish to express their sincere gratitude to Mr. J. H. Baik, general manager, quality assurance dept., Korea Heavy Industries and Construction Co., LTD, for the nuclear grade specimens, Mr. Y. Y. Kim, KINS, for the ferrite content meter, Mr. H. D. Cho and Dr. Y. S. Im , KAERI, for TEM microscopy and defects analysis, respectively, and Dr. H. W. Choi, KIGAM, for ion irradiation by accelerator. This work has been carried out as a part of the Reactor Pressure Boundary Materials Project under the Nuclear R&D Program by MOST, Korea.

References

[1] U. S. Nuclear Regulatory Commission Regulatory Guide 1.31, Control of Ferrite Content in Stainless Steel Weld Metal, Revision 3, April 1978.

[2] B. N. Singh and J. H. Evans, J. Nucl. Mater. 226 (1995) 277.

[3] Michio Kiritani, J. Nucl. Mater. 276 (2000) 41.

[4] A. Almazouzi, T. Diaz de la Rubia, B. N. Singh, M. Victoria, J. Nucl. Mater., 276 (2000) 295-296

[5] M. Victoria, N. Baluc, C. Bailat, Y. Dai, M. I. Luppo, R. Schaublin, B. N. Singh, J. Nucl. Mater., 276 (2000) 114.

[6] A. Iwase, S. Ishino, J. Nucl. Mater., 276 (2000) 178.

[7] Unpublished certified material test report, KHIC, 1998.

[8] ASTM E 521-96, Standard Practice for Neutron Radiation Damage Simulation by Charged-Particle Irradiation.

[9] A Study on the Influence of ä-Ferrite on the Irradiation Effects in Type 304 Stainless Steel Weldment, Yong-Kwan Shin, Master Thesis, SungKyunKwan University, 2000.

[10] K. Nordlung, F. Gao, Appl. Phys. Lett., submitted.

[11] W. Phythian, R. E. Stoller, A. J. E. Foreman, A. F. Calder, D. J. Bacon, J. Nucl. Mater., 223 (1995) 245.

[12] M. J. Caturla, N. Soneda, E. Alonso, B. Wirth, T. Diaz de la Rubia, J. M. Perlado, J. Nucl. Mater., 276 (2000) 13

[13] Y. N. Osetsky, D. J. Bacon, A. Serra, B. N. Singh, S. I. Goolubov, J. Nucl. Mater., 275 (2000) 65

[14] M. H. Loretto, R. I. Smallman, Defect Analysis in Electron Microscopy, pp. 77 – 88, Chapman and Hall, London (1975).

[15] G. R. Odette and G. E. Lucas, Proceedings of Ishino Conference, The university of Tokyo, 1994, p. 30.

Table 1 Chemical composition of Type 304 stainless steel (base metal) (wt%).

C	Ni	Cr	Mn	P	S	Si	N	Fe
0.045	**8.66**	**18.1**	**1.06**	**0.027**	**0.002**	**0.56**	**0.05**	**Bal.**

Table 2 Chemical composition of the filler metal for FN 8.5 weld (wt%).

C	Si	Mn	P	S	Ni	Cr	Cu	Mo	V	Cb+Ta	N	Ti	Fe
0.025	**0.78**	**0.97**	**0.022**	**0.003**	**9.54**	**19.5**	**0.12**	**0.08**	**0.08**	**0.011**	**0.064**	**0.019**	**Bal.**

Table 3 Chemical composition of the filler metal for FN 5.5 weld (wt%).

C	Si	Mn	P	S	Ni	Cr	Co	Cu	Mo	V	Cb+Ta	N	Ti	Fe
0.047	**0.698**	**1.146**	**0.023**	**0.003**	**10.72**	**20.66**	**0.09**	**0.15**	**0.12**	**0.07**	**0.001**	**0.056**	**0.02**	**Bal.**

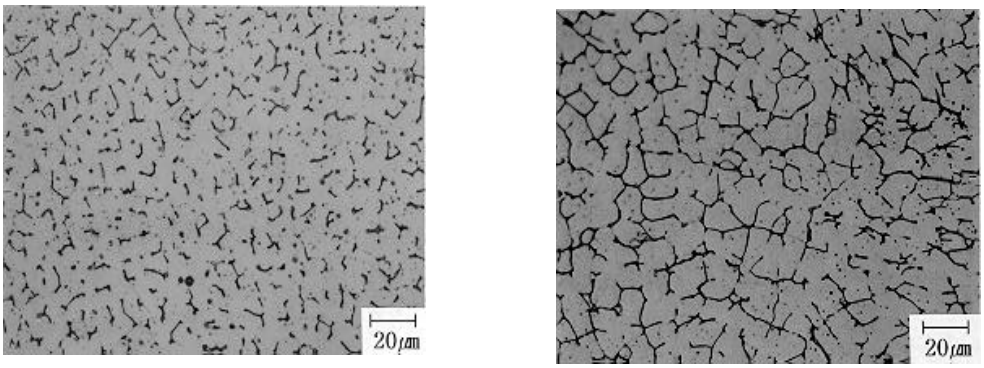

FN 5.5 **FN 8.5**

Fig. 1 As-received optical microstructure of FN 5.5 and FN 8.5 Type 304 stainless steel weldment.

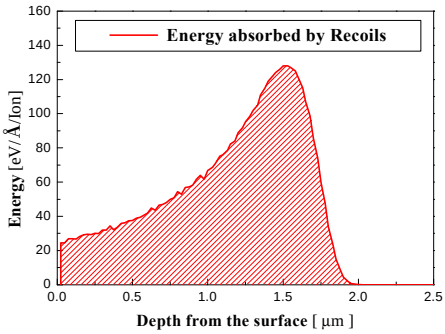

Fig. 2. TRIM 95 result on the Change of 8 MeV Fe^{+4}ion energy absorbed by recoil atoms with depth : Peak Damage Depth (Range): 1.5 μm. FWHM: 0.7 μm. FWHM: 0.7 μm

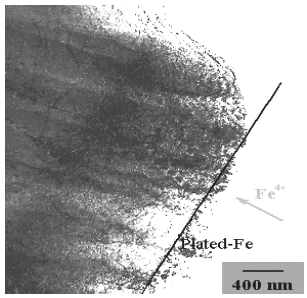

Fig. 3. Distribution of irradiation-induced defects. Peak damage and FWHM are seen to be about 1.5 μm and 0.7 μm, respectively.

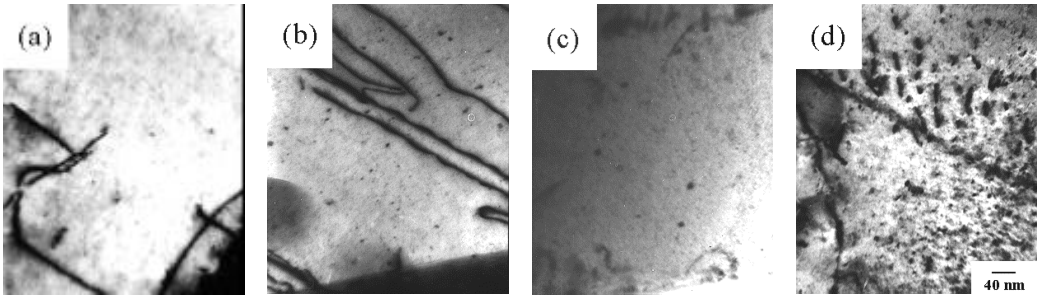

(a) δ-ferrite , 0 dpa (b) δ-ferrite, 1.5dpa. (c) austenite matrix , 0 dpa. (d) austenite matrix, 1.5dpa

Fig. 4. TEM microstructure for as-received and irradiated δ-ferrite and austenite matrix. Clear differences in the number and size of the irradiation-induced defects are seen between the bcc δ-ferrite and fcc austenite matrix.

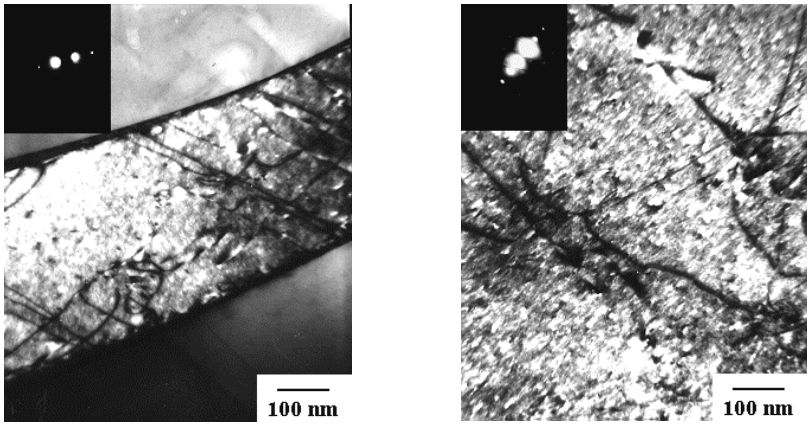

(A) δ-ferrite (B) Austenite matrix

Fig. 5 Defects analysis under two beam condition. It is seen that most of lines of contrast are perpendicular to $\bar{\mathbf{g}}$, the operating reflection. (A) BCC[$\bar{1}$11]zone,$\bar{\mathbf{g}}$ = [0$\bar{1}$1]. (B) FCC[$\bar{1}$12]zone,$\bar{\mathbf{g}}$ = [1 $\bar{1}$1].

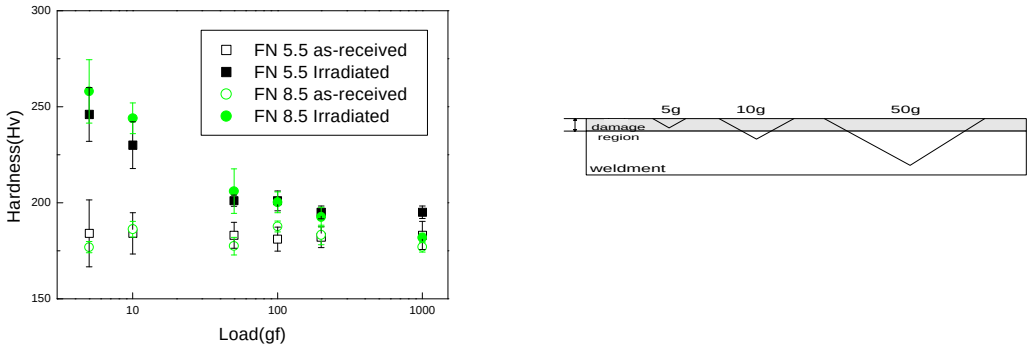

(A) **(B)**

Fig. 6 (A) Test load (5 ~ 1,000g) effects on the irradiation-induced Vickers microhardness in the as-received and irradiated FN 5.5 and 8.5 welds. **(B)** Relative position of the indentation with ion-damaged region.

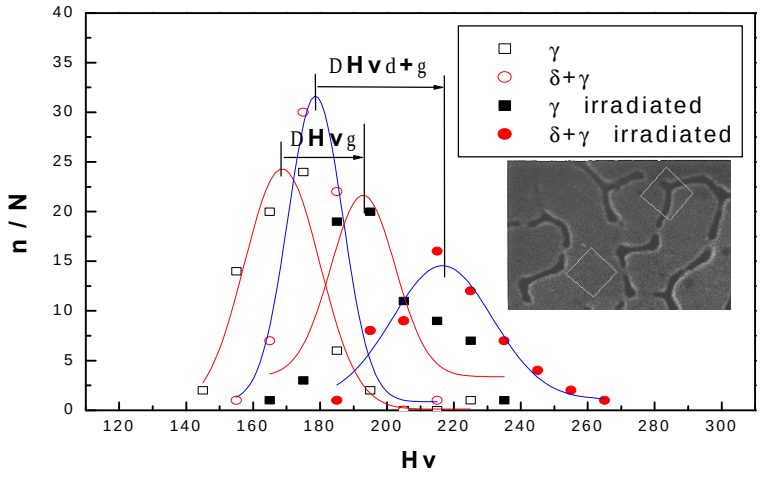

Fig. 7 Determination of phase contribution to the Vickers microhardness increase after irradiation.

The δ-ferrite area measured on the 70 indentations for irradiated welds of bcc δ-ferrite and fcc austenite matrix phases was about 25 % of the 5 g load indentations by image analyser

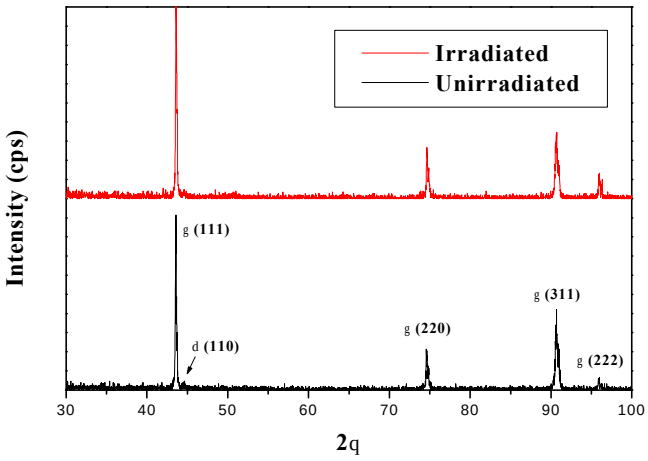

Fig. 8 X-ray diffraction spectra for type 304 stainless weldment in as-received and irradiated condition.